Archives of Current Research International

Volume 23, Issue 3, Page 42-52, 2023; Article no.ACRI.97753
ISSN: 2454-7077

Application of Deep Learning Techniques in the Development of Predictive Maintenance and Fault Detection in Electric Motors

Stanley Washington Ferreira de Rezende [a], Paulo Elias Carneiro Pereira [a], Bruno Pereira Barella [b], Alexsander Lindolfo Lima [b], Roberto Mendes Finzi Neto [a] and Jose dos Reis Vieira de Moura Jr. [b*]

[a] School of Mechanical Engineering, Federal University of Uberlandia, Uberlandia, Brazil.
[b] Institute of Mathematics and Technology, Federal University of Catalao, Catalao, Brazil.

Authors' contributions

This work was carried out in collaboration among all authors. All authors read and approved the final manuscript.

Article Information

DOI: 10.9734/ACRI/2023/v23i3564

Open Peer Review History:
This journal follows the Advanced Open Peer Review policy. Identity of the Reviewers, Editor(s) and additional Reviewers, peer review comments, different versions of the manuscript, comments of the editors, etc are available here: https://www.sdiarticle5.com/review-history/97753

Original Research Article

Received: 09/01/2023
Accepted: 17/03/2023
Published: 21/03/2023

ABSTRACT

During the last two decades, there has been remarkable growth in the processing capacity of computers and the evolution of digital cameras. As a result, the thermographic technique and thermal analysis became more applied in electromechanical maintenance due to the low measuring device cost. Simultaneously, new methods based on Deep Learning focused on image and video processing have emerged. In this sense, this contribution aims to verify the applicability of using the deep learning technique of convolutional neural networks to classify patterns of

**Corresponding author: Email: zereis@ufcat.edu.br;*

thermographic images of a bench grinder. The methodology used was the collection of thermographic pictures of a bench grinder after starting, without, and after applying loads to the discs. This procedure induced a temperature increase in the grinding machine housing since some types of faults in electric motors can be diagnosed due to over-temperature by thermographic inspection. Furthermore, a Python computational code was developed using a convolutional neural network to classify different grinder operation profiles based on thermal images. In conclusion, the technique proved promising for diagnosing motor failures by thermography and can be implemented in automatic predictive maintenance routines.

Keywords: Thermal analysis; thermography of electric motors; convolutional neural networks; intelligent maintenance system; industry 4.0.

1. INTRODUCTION

The development and use of monitoring systems capable of providing information about the operating state of the machinery and components play a critical role in a condition-based maintenance strategy, focusing on the operation's reliability and safety and reducing costs. In this context, and considering the need for a non-invasive approach, several non-destructive evaluation techniques were developed, such as eddy current, shearography, magnetic particles, acoustic emission, thermography, dye penetrant inspection, and ultrasonic and vibration-based methods.

Infrared thermography has been widely used in several situations due to its efficiency, cost, and possible integration into an intelligent monitoring system. Applications of the method include the monitoring of fouling in heat exchangers by Berce et al. [1], the development of cracks in construction stones by Vazquez and Thomachot-Schneider [2], and Hatir et al. [3] and the detection of delamination in reinforced concrete bridges by Ichi and Dorafshan [4]. In addition, Li et al. [5] developed a method to monitor defects in post-tensioned tendon ducts, Pearlman et al. [6] applied it to nuclear fuels inspection, and Matuzović et al. [7] used it as a tool to validate a heat transfer model of a roots blower.

Electric motors are used in several industrial segments. Detection of a failure in such types of machinery promptly provides a reliable and safe operation process and, beyond, avoids waste of sources [8]. Furthermore, the heat transfer phenomena in such machines can be used for failure detection by comparing the thermographic data at the non-damage and damage conditions, which enables the use of infrared thermography for fault detection purposes.

The infrared thermography was applied by Jeffali et al. [9] for failure detection in a 3-phase induction motor to monitor the fault propagation and detect degradation of components, whose results achieved 100% accuracy in all cases. Khanjani and Ezoji [8] developed a model for failure classification from thermographic data based on a convolutional neural network (CNN), k-means, and Support Vector Machine (SVM).

Infrared cameras have been combined with deep learning techniques for image recognition and damage classification for the automation process. One of these techniques, CNN, has already been used to monitor the conditions of rotating machines [10, 11]. Li et al. [11] proposed a CNN-based method for fault detection in rotating machines, whose results were superior to other methods, including the traditional vibration-based ones. Choudhary et al. [10] compared the results of CNN and regular multilayer perceptron (MLP) for fault detection in a rotating machine. The former presented better results, reaching an overall classification accuracy of 99.80%.

Et-Taleby et al. [12] developed a CNN-SVM mixed model for detecting and classifying faults in photovoltaic panels. CNN was used for feature extraction and SVM for classification. Two databases with different damage conditions were considered. The minimum accuracy obtained was 99.46%. Also, Mellit [13] built two classifiers based on CNN optimized and embedded into a low-cost microprocessor for fault detection and diagnosis in photovoltaic panels. The results showed 99.00% and 95.55% accuracy for fault detection and diagnosis, respectively. Likewise, Klamert et al. [14] applied a CNN model to curling failure detection in a Selective Laser Sintering (SLS) process, resulting average accuracy of 98.54%.

Kulkarni et al. [15] developed a deep-learning approach to detect sub-pavement voids caused by failing roadway culverts. They were based on images captured by an infrared camera installed in an unmanned aerial vehicle (UAV), and the results were comparable to those obtained by other traditional techniques. Also, in the same subject, Liu et al. [16] modeled crack identification and classification in asphalt pavement using Deep learning (DL) and infrared thermography. They considered four severity levels (no damage and three levels of crack development) and three image types (visible, infrared, and fusion of visible and infrared images). Results showed a better response for the DL applied to fusion images.

Woldeamanuel et al. [17] estimated the concrete strength in construction sites and laboratories by infrared images. They used a CNN model applied to true color and infrared images and reached anaccuracy higher than 80% concerning experimental results. Also, using the thermography data, the CNN approach represented a cost reduction of about 30% compared to the existing method. Finally, Zhou et al. [18] implemented a DL model for UAV thermal images to detect embankment leakage automatically. Results presented an overall accuracy of 94.90%, which showed that the approach has good applicability and generalization.

Picazo-Ródenas et al. [19] proposed a methodology based on data collected via infrared thermography to develop a model to calculate heat losses by convection and radiation through a 1.1 kW induction motor. Comparing a healthy machine and with rotor broken bars, they found that infrared thermography is an excellent tool for determining heating curves and energy balance under different motor conditions.

Schuss et al. [20] investigated the location of defects in photovoltaic panels with the help of synchronized thermography and time-resolved temperature. With the infrared images obtained, it was possible to identify the location of the defects as well as their influence on the output power losses.

Resendiz-Ochoa et al. [21] proposed failure analysis monitoring based on infrared images in induction motors and kinematic chains. Through the Otsu thresholding method, the extraction of thermal features was performed in some regions of interest. Using three failure conditions to demonstrate efficiency, namely, rotor broken bar, damaged bearing, and misalignment, it was possible to verify that this methodology effectively determines the intensity of failure conditions and their diagnosis.

Choudhary et al. [4] proposed an infrared thermography method based on emergent two-dimensional discrete wavelet transform to diagnose different bearing faults in an induction motor. After reducing the dimensionality and classifying the most relevant features, the resulting data were passed to three failure evaluation algorithms, complex decision tree (CDT), linear discriminant analysis (LDA), and support vector machine (SVM). With the results, it was possible to verify that the SVM was the one that best recognized bearing failures in induction motors [22].

Redon et al. [23] proposed a diagnostic tool for induction motors using infrared images and deep learning algorithms. After training, the classifier achieved good levels of accuracy concerning classification in the initial stages and the five scenarios considered (bearing lubrication failure, broken bars failures, fan failure, unbalanced failure, and healthy motor).

Following the monitoring of electrical motors, infrared thermography and CNN are used to detect failures in a grinding machine. The use of CNN allows the identification of modes of failure, and the approach can be used in an intelligent system, which provides quick responses so that decisions can be made promptly.

This proposal aims to demonstrate the viability of the joint use of CNN techniques with thermal analysis for follow-up and understanding of the behavior of failures in electric motors within a reduced context.

1.1 Infrared Thermography

The method is based on the thermal emissivity of a body being monitored, which indicates the capability of the material to emit energy as thermal radiation. This is a function of the material properties, wavelength, and temperature, once bodies with temperatures higher than absolute zero (0 kelvin) emit infrared radiation [6,4], whose wavelengths are between about 700 nm and 1 mm, not detected by the human eye [3].

The energy (E) emitted by a body is related to its temperature (T) through the Stefan-Boltzmann

equation (Eq. 1), where ε and σ refer to the emissivity and the Stefan-Boltzmann constant (5.6704×10^{-8} W/m^2·K), respectively [4,24].

$$E = \varepsilon\sigma T^4 \quad (1)$$

From the infrared radiation measured by infrared thermographic cameras, it is possible to establish the temperature profile of a body. Differences in temperature gradients in the target indicate the presence of discontinuities in the form of pits, craters, cracks, or internal voids; once those induce a faster cooling and heating about the surrounding area, making it possible to detect them by the proper treatment of the thermograms [6].

Infrared thermography (IRT) inspections can be performed by passive and active approaches. In the first method, the material being monitored is evaluated in qualitative terms, providing information about the presence or not of defects. However, in the latter approach, the target is excited by a source (e.g., laser, microwave), which results in its heating or cooling, thus making it possible to obtain quantitative data since the heating or cooling features of the excited source are characterized [2,4,25]. Nevertheless, the active approach is less applied than the passive one due to its complexity, mainly in monitoring structures in the field.

1.2 Convolutional Neural Networks

Several Machine and Deep Learning techniques have been used in conjunction with monitoring techniques in recent years [26-29]. CNN is a deep learning technique capable of extracting the features and differentiating the data between several conditions, being used for a wide range of image classifications [11]. A CNN model consists of several layers, among which the main ones are convolution and fully connected. In the beginning, it contains a set of filters that performs the extraction of the features of the input images according to a selected kernel. Then, flattening operations and dense layers integrate the features extracted from the previous layers. This results in a feature vector for classification, whose dimensions are related to the number of classes to be classified [10,11,30].

In a traditional structure of a CNN model, the convolutional layer is followed by a batch normalization one, which reduces the shift of internal covariance, accelerating the training process of the deep network. Also, the convolution layer can be succeeded by an activation consisting of nonlinear functions (e.g., hyperbolic tangent, sigmoid, and Rectified Liner Unit - ReLU), aiming to accelerate the convergence of the CNN. In the sequence, usually, it's defined a pooling layer where it's done the reduction of the dimensions of the obtained feature map in the function of the pooling size and the selected method (e.g., maximum, average, or summation pooling), keeping constant the feature map count, reducing the calculation cost and controlling the over-fitting. Next, it's linked to the fully connected layer and the softmax regression, which performs a probabilistic classification [10,11].

2. METHODOLOGY

To evaluate the deep learning technique associated with thermographic analysis, an experimental procedure was proposed to overheat an electric motor in a controlled manner without causing permanent damage to the equipment. Thus, the electric motor used was a bench grinder, as shown in Fig. 1. To modify the temperature profile of the motor, a resistive load was applied to rotation on the right axis of the equipment.

Fig. 1. Bench grinder used in the overheating study

An HTI thermographic camera, model HT02, with an image resolution of 60x60 (3600 pixels), was used to obtain thermographic images. The following parameters were used for image acquisition: Ambient temperature: 27°C (measured with another thermometer); Emissivity: 0.95 (painted metallic surface, according to the device manual); Relative air humidity: 21%.

After acquiring several photos in the two operating conditions of the grinder: without load and with load, they were used to train a condition classification model based on a convolutional neural network. This neural network was responsible for evaluating the standard temperature profiles for each operational condition of the grinder.

However, a primary pre-processing step was required before building a classification model. Fig. 2 presents the images obtained during the experimental procedure for collecting thermographic photographs.

As can be seen in general, the images obtained by thermography allow the identification of two different temperature profiles of the monitored component subjectively and humanly. Since the temperature profiles are already sufficient to interpret the equipment's stress condition clearly in this work, the color tones were not readjusted in scale.

This procedure should be performed if both behaviors had very similar temperature profiles during the data sampling process but with different scales and temperature ranges. This type of thermographic camera automatically adjusts the color tones to the range of temperatures occurring on the screen. If the motor presented a similar image for both conditions, varying the temperature range, for example, from 28 to 35 °C for the no-load case but 40 to 50 °C for the load condition, it would be necessary to normalize the data to that both color profiles look distinct. This additional task would not add relevant complexity because there are already several normalization and standardization functions in the sci-kit learn library, also used in this contribution for the data separation step in training and testing.

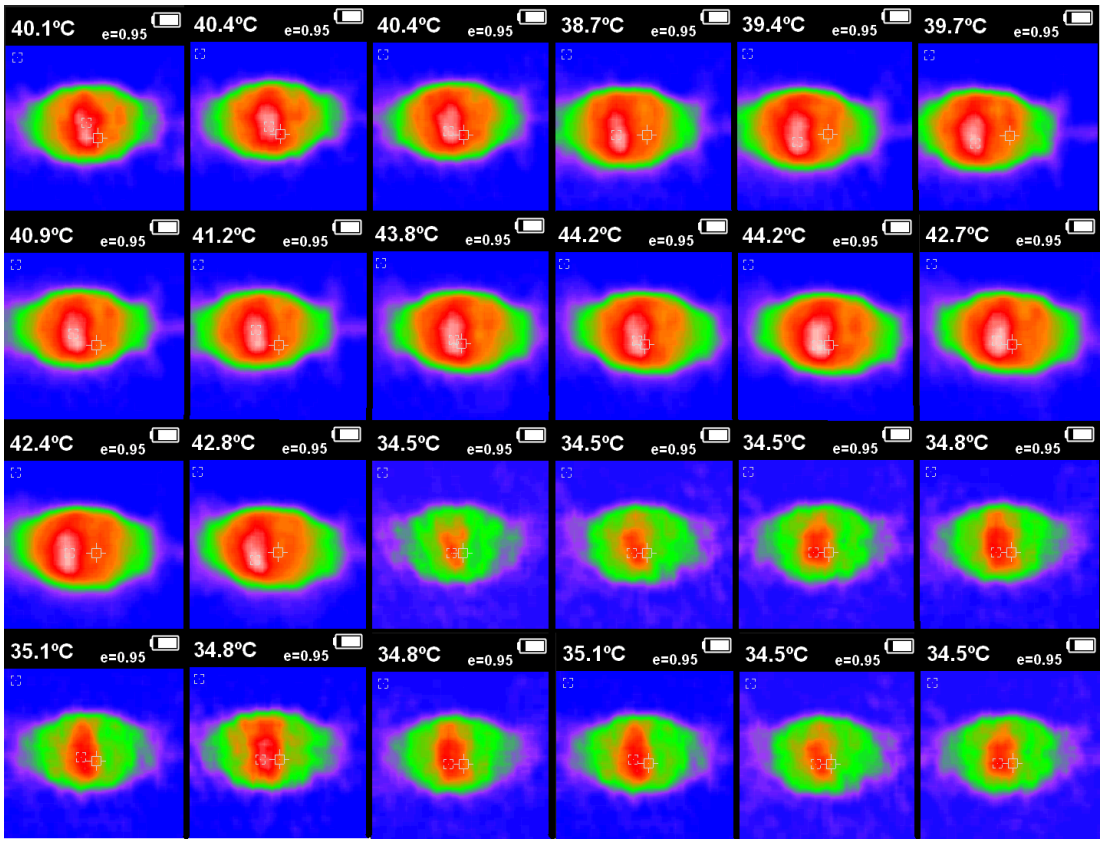

Fig. 2. Some thermographic images obtained from the bench grinder with and without load

Since the raw data, in this case, were based on manual collections from a portable device, a data pre-processing step was necessary. The images were initially converted from the standard three-layer RGB (red, green, blue) to a single layer of 256 shades of gray. Then, the image removes the header and footer with information not used for the model's decision-making because it is not part of the thermal image of the electrical motor. Fig. 3 illustrates a thermographic image obtained and the superimposition of the motor to visualize its positioning.

In Fig. 3, it is possible to see the option of the camera to superimpose the thermal images on the actual image of the object to facilitate the positioning of the tripod to take pictures. However, due to the low mass of the bench, it suffered small displacements from the base caused by engine rotation. Nevertheless, this noise did not impact the classification step of the temperature profiles.

Still, in Fig. 3, there is no significant color variation when it is turned off or at the beginning of the motor rotation. To reinforce this point, Fig. 4 is presented, a photo taken shortly before Fig. 3, removing the overlap of the actual image.

As expected, Fig. 4 presents a homogeneous color pattern since the motor is turned off and its temperature is in thermal equilibrium with the environment. After a few seconds of rotation, the motor overheats forming the temperature profile without applying load.

As can be seen from the color scale at the bottom of the thermal pictures and by overlay, the green temperature profile still represents a lower temperature pattern, with the center of the motor experiencing the most heating. If the motor had some leakage of charges, wear, or increasing friction in rotation close to the bearings, these details would also represent hot spots in the images. However, the limited and non-destructive procedure adopted in this study was limited to applying a frictional load on the axis on the right side of the image, promoting a greater demand on the motor and thus causing overheating in Fig. 2.

Fig. 3. Image taken by the thermographic camera

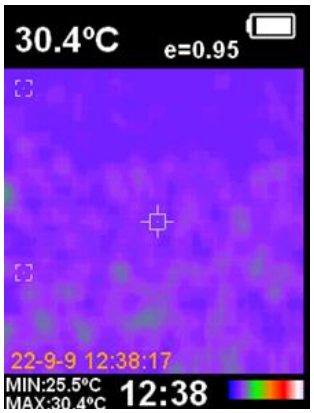

Fig. 4. Thermographic image at the start of the electric motor

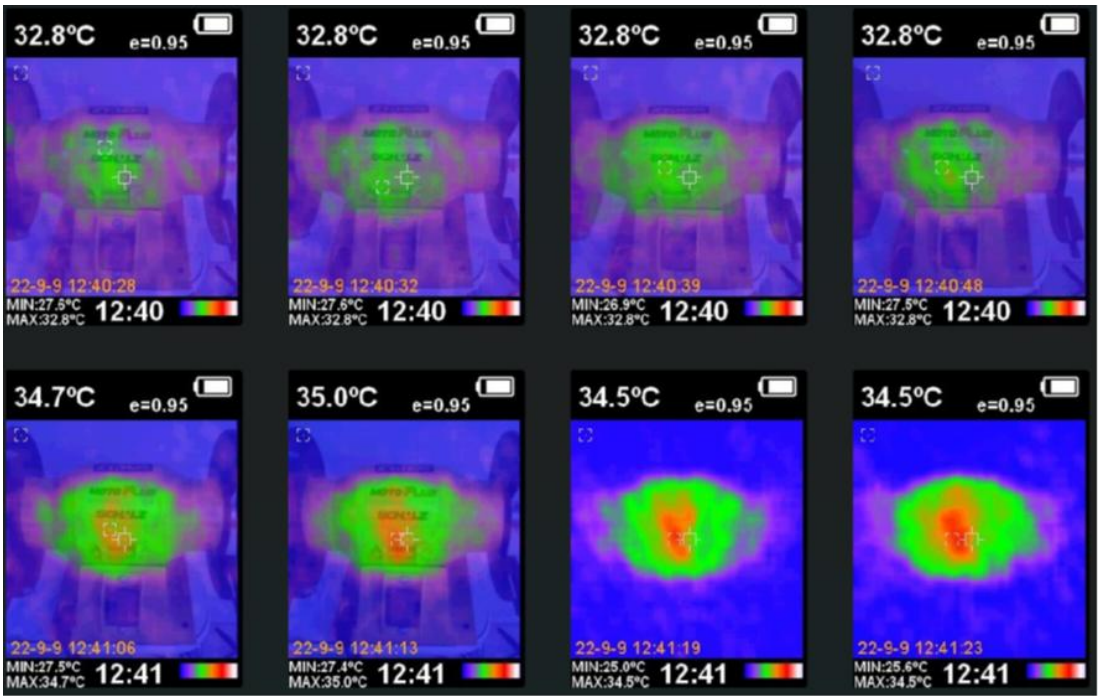

Fig. 5. Thermographic photos showing the temperature evolution of the engine at rest until the operation without load

A binary classification model based on convolutional neural networks was constructed with images obtained from loaded and unloaded profiles on the grinder. Images obtained after pre-processing were used as input parameters for the model. This pre-processing first consisted of transforming the RGB color pattern (three layers of colors) into one of 256 levels of gray. Then remove the header and footer from the image shown in Fig. 3. Fig. 6 illustrates this sequence of pre-processing steps.

After pre-processing the sample images, the model based on a convolutional neural network was implemented using the Keras library recently included within TensorFlow for Python language and is discussed in the next section.

3. RESULTS AND DISCUSSION

The CNN-based model uses 256 grayscale images in a 160x240 pixel matrix as inputs. The model's topology comprised three 2D convolutional layers, with 32, 64, and 64 neurons, respectively. In all of them, the activation function was ReLU using weight initialization by the Uniform He function. After performing the resizing by a Flatten layer, the model connects to a fully connected layer with 100 neurons and is then directed to another output layer with only two neurons. In this last layer, a Softmax activation function was used due to the classification decision-making process, indicating the percentage of chances of being included in the group of images without or with the load.

The model still used the k-fold evaluation process in which ten executions of the entire process were carried out to survey the metrics and adjustments of the model to ensure its convergence and optimal results. The model's result metric was accuracy (the ability to predict correctly), and the loss function used for the training process was categorical cross-entropy, as it is a classification process.

Of the total set of 240 samples, 100 images without load and 140 with load, 33% of the data were used for testing and the rest for model training.

Thirty epochs of training were performed in each execution, using batches of size 3 for readjusting the weights. The optimization function used in the training process was ADAM, an algorithm with an adaptive learning rate. This function is generally used because it has a lower computational time for convergence in gradient-based problems, in addition to a smaller number of parameters for calibration, and is based on two other established techniques: AdaGrad and RMSProp. Fig. 7 presents the loss function and accuracy graphs along the training steps.

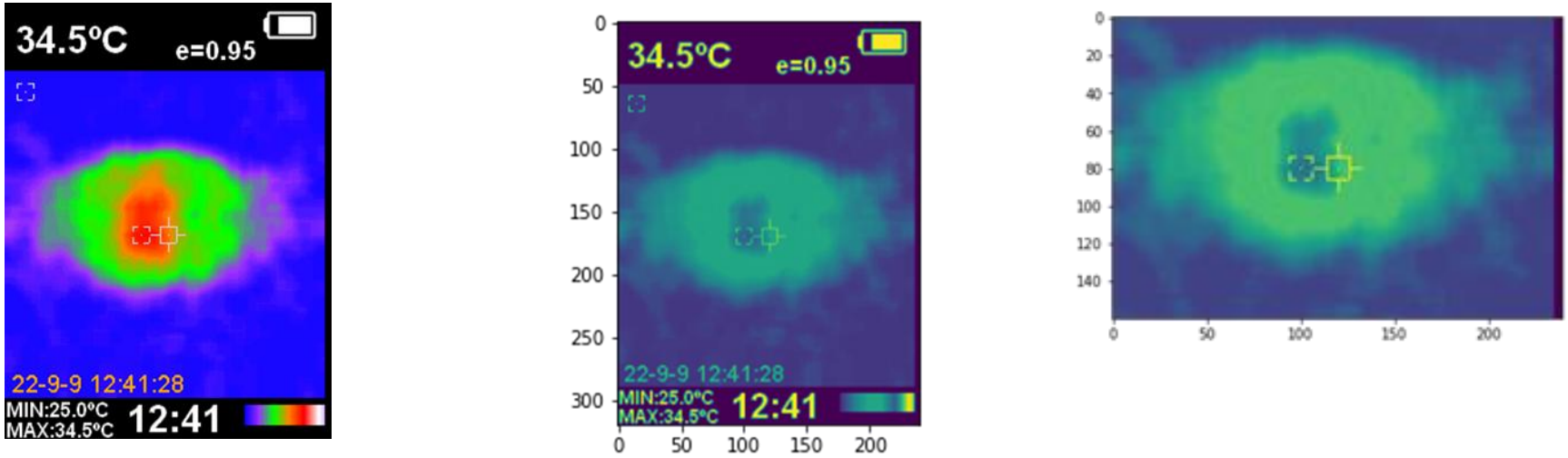

a) Original picture b) Color change c) Window selection

Fig. 6. Pre-processing of images with header and footer removal

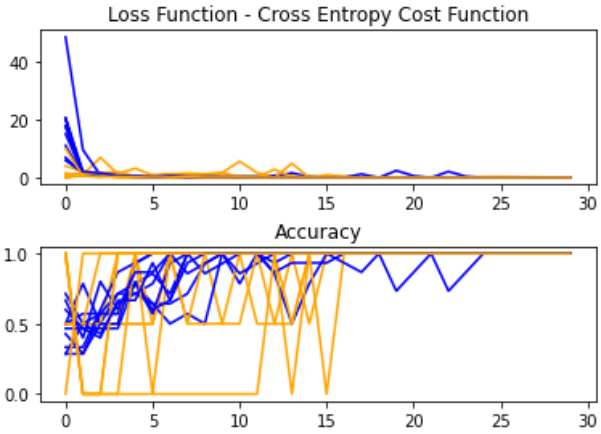

Fig. 7. Results obtained with the CNN model

The curves in blue are training data, and in orange are test data. The Loss Function only makes sense in the training stage because it adjusts the weights. However, during this modeling step, it is common to present test and training data for verification. In both cases, in the loss function graph, it is possible to see that the values achieved converge to low values over the epochs, tending to zero when they reach epoch 10.

In the accuracy graph, it is possible to notice a hit of 1.0 (100%) for both training and test data after 20 epochs. This shows that after building the model, it has obtained a capacity of 100% of the correctness of an image, correctly classifying it between a motor with load or without.

For this type of evaluation of a binary classification model, it is common to use a confusion matrix illustrating the results. However, due to the results achieved with the model, with a clear distinction between the monitored conditions, there were no false positives or negatives (type I and II errors). Therefore, representing this result in a confusion matrix is unnecessary.

4. CONCLUSION

Maintenance has always been one of the highest costs in the industrial environment. However, in recent years, a greater demand for planning and availability of equipment associated with the new concepts of industry 4.0 has increased the capacity and need for maintenance. As a result, the idea of prescriptive maintenance emerges with Industry 4.0. It increases the level of Predictive Maintenance requests, monitoring the condition of items and reconciling with concepts of IoT, Big Data, Cloud Computing, and Artificial Intelligence.

As already mentioned, the study in question qualitatively showed at the beginning that the engine temperature patterns under load and no load conditions were different, facilitating the pre-processing step. In addition, the number of evaluated conditions was limited to non-destructive equipment conditions, as they were only assessed with and without load application to cause overheating. In this way, the reduced set of samples was also facilitated. Of course, for conditions in which different sources of damage are sought to be evaluated, such as leakage of electrical charges dissipating and promoting the joule effect or wear in bearings causing friction, new destructive cases in the equipment are necessary. Still, the temperature profile is expected to differ from the two already presented here. Thus, the assumptions and procedures used in this study will also apply under these conditions.

As for the model obtained, some characteristics that may suggest overfitting can be noticed. This is due to the reduced number of samples used in the study, which was also justified by the low qualitative variability between samples. However, as the accuracy graph shows, after more iterations, the test sets also tend to obtain the same results as the training sample group.

COMPETING INTERESTS

Authors have declared that no competing interests exist.

REFERENCES

1. Berce J, Zupančič M, Može M, Golobič I. Infrared thermography observations of crystallization fouling in a plate heat exchanger. Appl Therm Eng. 2023;224: 120116.
   DOI:10.1016/j.applthermaleng.2023.120116.
2. Vazquez P, Thomachot-Schneider C. Infrared thermography as a tool to detect increasing cracking in granitic stones exposed to high temperatures. J Cult Herit. 2023;59:163-70.
   DOI 10.1016/j.culher.2022.11.015.
3. Hatir ME, İnce İ, Bozkurt F. Investigation of the effect of microclimatic environment in historical buildings via infrared thermography. J Build Eng. 2022;57: 104916.
   DOI 10.1016/j.jobe.2022.104916.
4. Ichi E, Dorafshan S. Effectiveness of infrared thermography for delamination detection in reinforced concrete bridge decks. Autom Constr. 2022;142:104523.
   DOI 10.1016/j.autcon.2022.104523.
5. Li S, Han S, Wang J, Han X, Zheng P, Cui C et al. Infrared thermography detection of grouting defects in external post-tensioned tendon ducts under construction hydration heat excitation. NDT E Int. 2023; 134:102785.
   DOI 10.1016/j.ndteint.2022.102785.
6. Pearlman M, Lupercio A, Rektor A, Lamb J, Fleming A, Jaques B et al. Infrared thermography method to detect cracking of nuclear fuels in real-time. Nucl Eng Des. 2023;405:112196.
   DOI 10.1016/j.nucengdes.2023.112196.
7. Matuzović M, Rane S, Patel B, Kovačević A, Tuković Ž. Analysis of conjugate heat transfer in a roots blower and validation with infrared thermography. Int J Thermofluids. 2022;16:100234. DOI 10.1016/j.ijft.2022.100234.
8. Khanjani M, Ezoji M. Electrical fault detection in three-phase induction motor using deep network-based features of thermograms. Measurement. 2021;173: 108622.
   DOI 10.1016/j.measurement.2020.108622.
9. Jeffali F, Ouariach A, Kihel BE, Nougaoui A. Diagnosis of three-phase induction motor and the impact on the kinematic chain using non-destructive technique of infrared thermography. Infrared Phys Technol. 2019;102:102970.
   DOI 10.1016/j.infrared.2019.07.001.
10. Choudhary A, Mian T, Fatima S. Convolutional neural network based bearing fault diagnosis of rotating machine using thermal images. Measurement. 2021;176:109196.
    DOI 10.1016/j.measurement.2021.109196.
11. Li Y, Du X, Wan F, Wang X, Yu H. Rotating machinery fault diagnosis based on convolutional neural network and infrared thermal imaging. Chinese J Aeronaut. 2020;33(2):427-38.
    DOI 10.1016/j.cja.2019.08.014.
12. Et-taleby A, Chaibi Y, Allouhi A, Boussetta M, Benslimane M. A combined convolutional neural network model and support vector machine technique for fault detection and classification based on electroluminescence images of photovoltaic modules. Sustain Energy, Grids Netw. 2022;32:100946.
    DOI 10.1016/j.segan.2022.100946.
13. Mellit A. An embedded solution for fault detection and diagnosis of photovoltaic modules using thermographic images and deep convolutional neural networks. Eng Appl Artif Intell. 2022;116:105459.
    DOI 10.1016/j.engappai.2022.105459.
14. Klamert V, Schmid-Kietreiber M, Bublin M. A deep learning approach for real time process monitoring and curling defect detection in Selective Laser Sintering by infrared thermography and convolutional neural networks. Procedia CIRP. 2022; 111:317-20.
    DOI 10.1016/j.procir.2022.08.030.
15. Kulkarni NN, Raisi K, Valente NA, Benoit J, Yu T, Sabato A. Deep learning augmented infrared thermography for unmanned aerial vehicles structural health monitoring of roadways. Autom Constr. 2023;148:104784.
    DOI 10.1016/j.autcon.2023.104784.
16. Liu F, Liu J, Wang L. Asphalt pavement fatigue crack severity classification by infrared thermography and deep learning. Autom Constr. 2022;143:104575.
    DOI 10.1016/j.autcon.2022.104575.
17. Woldeamanuel MM, Kim T, Cho S, Kim H-K. Estimation of concrete strength using thermography integrated with deep-learning-based image segmentation: Case studies and economic analysis. Expert Syst Appl. 2023;213:119249.
    DOI 10.1016/j.eswa.2022.119249.
18. Zhou R, Wen Z, Su H. Automatic recognition of earth rock embankment

leakage based on UAV passive infrared thermography and deep learning. ISPRS J Photogramm Remote Sens. 2022;191: 85-104.
DOI 10.1016/j.isprsjprs.2022.07.009.

19. Picazo-Ródenas MJ, Royo R, Antonino-Daviu J, Roger-Folch J. Use of infrared thermography for computation of heating curves and preliminary failure detection in induction motors. 2012 XXth International Conference on Electrical Machines, Marseille, France. 2012;525-531.
DOI: 10.1109/ICElMach.2012.6349920
20. Schuss C et al. Detecting defects in photovoltaic panels with the help of synchronized thermography. In IEEE Transactions on Instrumentation and Measurement. 2018;67(5):1178-1186.
DOI: 10.1109/TIM.2018.2809078
21. Resendiz-Ochoa E, Osornio-Rios RA, Benitez-Rangel JP, De J Romero-Troncoso R, Morales-Hernandez, "Induction Motor Failure Analysis: An Automatic Methodology Based on Infrared Imaging LA. In IEEE Access. 2018;6: 76993-77003.
DOI: 10.1109/ACCESS.2018.2883988.
22. Choudhary A, Goyal D, Letha SS. Infrared thermography-based fault diagnosis of induction motor bearings using machine learning. In IEEE Sensors Journal. 2021; 21(2):1727-1734.
DOI: 10.1109/JSEN.2020.3015868.
23. Redon P, Rodenas MP, Antonino-Daviu J. Development of a diagnosis tool, based on deep learning algorithms and infrared images, applicable to condition monitoring of induction motors under transient regime. IECON 2020 The 46th Annual Conference of the IEEE Industrial Electronics Society, Singapore. 2020; 2505-2510.
DOI: 10.1109/IECON43393.2020.9254639
24. Carvalho JP, Lamim PCM, Araujo ACS, Oliveira JF, Moreira JS. Parâmetros Relevantes Na Análise Termográfica De Um Motor de Indução Trifásico. In 14° Simpósio Brasileiro de Automação Inteligente – SBAI. 2019;649-53.
DOI 10.17648/sbai-2019-111206.
25. Avdelidis NP, Moropoulou A. Applications of infrared thermography for the investigation of historic structures. J Cult Herit. 2004;5(1):119-27.
DOI 10.1016/j.culher.2003.07.002.
26. Rezende, SWF, Moura Jr, JRV, Neto, RMF, Gallo, CA, Steffen Jr, V. Convolutional neural network and impedance-based SHM applied to damage detection. Engineering Research Express. 2020;2:035031.
DOI 10.1088/2631-8695/abb568
27. Rezende STF, Barella BP, Moura Jr. JRV. Damage identification of vehicle brake disks by the use of impedance-based shm and unsupervised machine learning method. International Journal of Advanced Engineering Research And Science. 2020;7:324-330.
DOI 10.22161/ijaers.76.40
28. Freitas, FA, Jafelice, RM, Silva, JW, Rabelo, DS, Nomelini, QSS, Moura Jr, JRV, Gallo, CA, Cunha, MJ, Ramos, JE. A new data normalization approach applied to the electromechanical impedance method using adaptive neuro-fuzzy inference system. Journal of the Brazilian Society of Mechanical Sciences and Engineering. 2021;43:1-20.
DOI 10.1007/s40430-021-03186-z.
29. Gonçalves, DR, Moura Jr., JRV, Pereira, PEC, Mendes, MVA, Diniz-Pinto, HS. Indicator kriging for damage position prediction by the use of electromechanical impedance-based structural health monitoring. Comptes Rendus. Mécanique. 2021;349:225-240.
DOI: 10.5802/crmeca.81.
30. Ornek AH, Ceylan M, Ervural S. Health status detection of neonates using infrared thermography and deep convolutional neural networks. Infrared Phys Technol. 2019;103:103044.
DOI 10.1016/j.infrared.2019.103044.

© 2023 Rezende et al.; This is an Open Access article distributed under the terms of the Creative Commons Attribution License (http://creativecommons.org/licenses/by/4.0), which permits unrestricted use, distribution, and reproduction in any medium, provided the original work is properly cited.

Peer-review history:
The peer review history for this paper can be accessed here:
https://www.sdiarticle5.com/review-history/97753